International Journal of Developmental Neuroscience 68 (2018) 106–110

Contents lists available at ScienceDirect

International Journal of Developmental Neuroscience

journal homepage: www.elsevier.com/locate/ijdevneu

Deciphering brain-specific transcriptomic expression of *Ezr*, *Rad* and *Msn* genes in the development of *Mus musculus*

Syed Aoun Ali, Deeba N Baig*

Department of Biological Science, Forman Christian College (A Chartered University), Zahoor Elahi Road, Lahore, 54600, Pakistan

ARTICLE INFO

Keywords:
Ezrin
Radixin and moesin

ABSTRACT

Ezrin, Radixin and Moesin (ERM) are critical membranous component involved in cross-linking of actin filaments. Moesin (*Msn*) is recognized as a pivotal protein involved in regulation of cell signalling events associated with the maintenance of epithelial integrity, actin organization and polarity. Radixin (*Rad*) is known to cell-to-cell adherens junction as a barbed end-capping protein whereas ezrin (*Ezr*) is recognized at cell adhesion, motility, apoptosis and phagocytosis. The current study for the first time reports the transcriptional and RNA secondary structural variations among brain-specific ERM genes. Firstly, we analyzed brain-specific transcriptomic expression in selected embryonic and postnatal developmental stages (E10.5, E14.5, E18.5, P0.5, P3.5, P5.5, P10.5 and P20.5) of *Mus musculus*. Among designated developmental stages, *Ezr* has highest fold difference in early embryonic and postnatal stages (E10.5, P0.5 and P5.5). *Rad* showed a similar pattern of high expression especially at embryonic stages (E10.5 and E18.5) and postnatal (P0.5 and P5.5), however, *Msn* exhibited non-significant fold differences in comparison to controls leading to its curial role in development. Furthermore, computational prediction of ERM coding mRNA transcripts, reveals compact and less dynamic *Msn* secondary structure and pseudoknots configurations, in contrast to *Ezr* and *Rad*. Conclusively, transcriptomic levels are greatly associated with compact base pairing organization of its secondary structures. These findings open a new domain to understand the occurrence of ERM-specific cytoskeleton proteins during developmental stages.

1. Introduction

The cytoskeleton is the most diverse cellular network of the cell. It is an intricate communication of microfilaments and microtubules in the cytoplasm that controls cell shape, maintains intracellular organization, and in cellular mobility (Goldman et al., 2008). Among cytoskeleton molecules, least is known about ERM members. the role of ERM proteins is recently highlighted in cellular environmental microfilaments (Thomas, 2011) and found to be crucial in cellular migration and proliferation, this finding provided information in the involvement of ERM members in cancer and in serval neurological disorders (Yaming et al., 2015). Previously, ezrin (*Ezr*) 81-KDa was identified as a constituent of chicken microvilli (Bretscher, 1983) later on also found in lungs, kidneys, epithelial and mesothelial cells (Louvet-Vallée, 2000). *Ezr* found cytosolic proteins which are present in the juxtamembrane region. The localization of *the Ezr* protein is evident for its dynamic activity and cellular actions (Sarrió et al., 2006). The second member of ERM family radixin (*Rad*) 82-KDa was first isolated from mammalian hepatocytes and has found end-capping actin-modulating protein (Amieva et al., 1994). Interestingly, *Rad* molecule was noticed on synaptic membrane interaction with GABAA receptors. Thus, indirectly involved in neuronal regulation (Loebrich et al., 2006). Moesin (*Msn*) 78-KDa is a heparin-binding protein and was identified as third ERM members as membranous protrusions and involve in cell growth regulation and mobility. The cellular movement is also greatly influenced by the localization of mRNA within the cell which creates a cellular polarity for different transportational and cytoskeleton proteins to be synthesis at various ends of the cellular structure. Along with abundant evidence of proteins sorting and selective transportation to different polarized areas of cell, an increasing volume of evidence have suggested a promising role of mRNA concentration at respective positions with their secondary and tertiary structures influence have been reported. (Liao et al., 2015). Therefore, we explored ERM member's co-transcriptional levels in *Mus musculus* brain tissues and their mRNA sequence's secondary structures by using computational biology servers, which are directly and indirectly involved in most of cellular signalling and survival processes such as cell division, adhesion, polarity, migration and cellular movement facilitated by cytoskeletal proteins

* Corresponding author.
E-mail address: deebabaig@fccollege.edu.pk (D.N. Baig).

https://doi.org/10.1016/j.ijdevneu.2018.06.003
Received 26 December 2017; Received in revised form 11 June 2018; Accepted 11 June 2018
Available online 12 June 2018

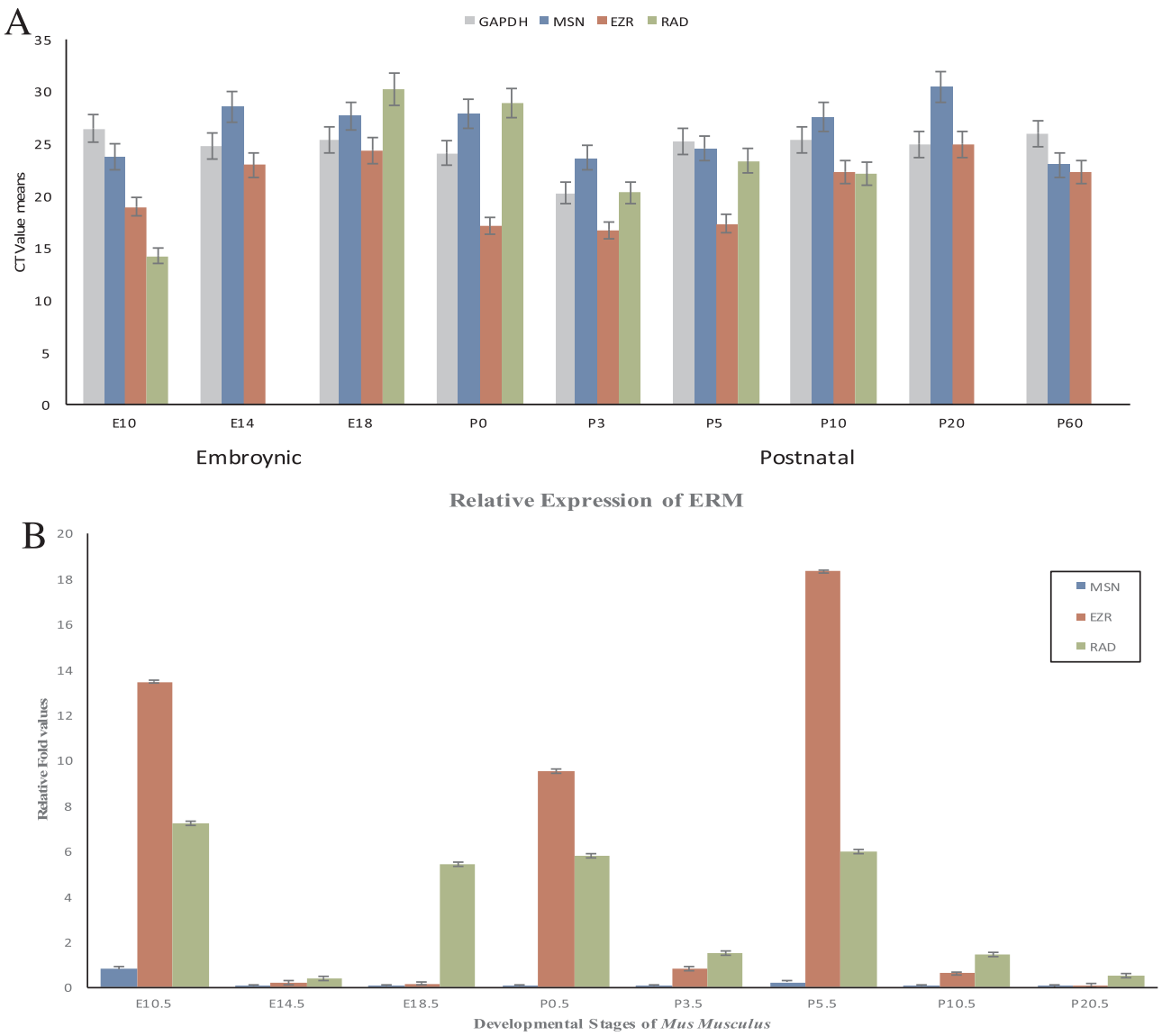

Fig. 1. ERM transcriptional expression, A.CT value means based expression profile. B. Fold chart by using ΔΔCT value analysis.

(Thomas, 2011).

2. Results

Transcriptional analysis of ERM genes in *Mus musculus* pre and postnatal brain developmental stages was done. The expression levels of each member were normalized with GAPDH. Statistical analysis by One way ANOVA, revealed variable significance level for ERM members, *Msn* and *Ezr* were significantly expressed in all selected stages. However, expression of *Rad* was significant in most of the selected stages other than P20.5 and P60.5, where it was highly non-significant (Fig. 1A).

Transcriptional fold differences were shown variably by all genes analyzed compared with calibrator (P60.5) and normalized against GAPDH. Expression of *Msn* remained significantly similar throughout all experimental stages overlying its curial importance and presented much stable expression. Whereas *Ezr* exhibited significant expression fold at E10.5 among embryonic stages and at P0.5 and P5.5 postnatal stages. *Rad* expression shows fold increase at embryonic stages (E10.5 and E18.5) and postnatal (P0.5 and P5.5). ERM expression fold analysis imprints the competitive roles of *Ezr* and *Rad* with each other however *Msn* expression has minimum variability (Fig.1B).

The RNA quantitation is depend on its stability and integrity. RNA secondary architecture structure is more conserved parameter than primary sequence, specifically for protein encoding RNA molecules and whose function depends on their structure. The approach has been utilized based on the fold and align method by using NUPACK online server (MIT, USA). Selected secondary structures were thermodynamically stable and determined on the basis of lowest free energies (minimum ΔG for *Ezr*, *Msn* and *Rad*, -492 kcal/mol, -480.80 kcal/mol and -382.20 kcal/mol respectively). ERM transcripts secondary structures were extensively variable in folding configurations which exhibits distinct mismatches, multi-branches and loops along with psudoknots. Fig. 2. also present psudo-knotted structures, which are further elucidated in the graphical presentation in Fig.3. ProbKnot algorithm predicts ERM mRNA sequence on the bases of most probable base pairing within their sequences and with themselves. Each pseudoknot based mRNA transcript configuration represents probable base pairing for each member of ERM. *Ezr* and *Rad* have a less pseudoknots in the transcripts, whereas, *Msn* shows much scattered and extensive psudoknotted structures. Hence, the distinct presence of psudoknots in transcripts effected on the integrity of molecule. Structural evidences of transcripts support the variability in expression patterns of ERM members in selected developmental stages.

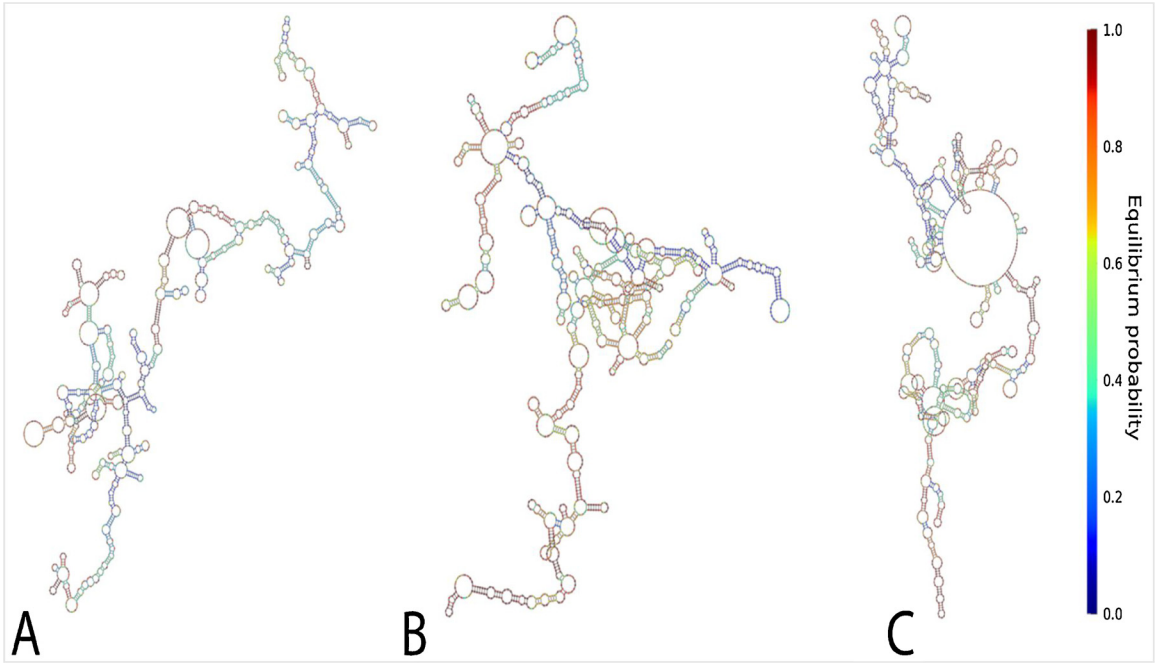

Fig. 2. Stem and loop based RNA secondary structures. (A) *Ezr*, (B) *Msn*, (C) *Rad*.

3. Discussion and conclusion

ERM genes are found to be very important genes involved in many cellular processes and act as a major cytoskeleton component. ERM works with actin filaments and helps in maintaining cell shape and movement mostly. Since their role in cell's physical attributes, they have been extensively explored throughout scientific reports towards their clinical importance and relevance with promising results towards their future use in therapeutics. It has been validated that two of the ERM genes (*Ezr* and *Msn*) have been responsible for mammalian brain development as *Ezr* is expressed in radial glia area and in parental human cerebrum where migration of cells takes place towards intermediate zones, whereas *Msn* is expressed in vascular endothelial cells in developing brain tissues by conducting immunohistochemical studies in tuberous sclerosis (TSC) which are non-cancerous tumors. *Ezr* and *Msn* have shown co-localization with tuberin and hamartin which are major two genes for TSC (Johnson et al., 2002). In another medical scientific report, the role of ERM genes was exploited with their property of controlling cellular shape, motility and supporting proliferation. Tissues microarrays conducted on Squamous cell carcinoma (SCC) samples revealed the greater correlation of high levels and subcellular localization of ERM proteins proofs their role in cell physical dynamics which helps tissues towards organogenesis by their direct involvement in cell movement and proliferation (Madan et al., 2006). ERM role in controlling cell movement have been illustrated in traumatic brain injury where rapid movement of microglial cells and peripheral macrophages rushes towards injury point. This phenomenon is being medicated by migration of immune cells, which are influenced by actin cytoskeleton protein. The high expression of ERM depicts their direct role in supporting actin filaments to help cellular movement (Younghyeb et al., 2011). Radixin among ERM has a different role in cellular dynamics, as it plays the role on the surface of cells and causes a cell to cell adhesion. It was further proofed in the migration of PC3 prostate cancer cells where *Ezr* and *Msn* both have been depleted by RNA interference, whereas only *Rad* allowed functioning which caused the development of adherens junctions between cell to cell connections and an overall increase in cell spread was observed. Whereas *Rad* depletion causes altered actin organization, which combines the role of ERM genes together for the functioning of actin filaments (Valderrama et al., 2012).

The variable expression fold differences of *Ezr* and *Rad* in developing brain tissues, suggest the connection of their role in migration of cells whereas high levels of *Rad* at birth stages (E18.5 and P0.5) shows its role in cell to cell function which lead to tissues maturation with its departing fold expression in later stages, whereas *Ezr* showing much significant fold difference not only at birth stages but also in early development (E10.5) and in later postnatal stages (P5.5) indicates its

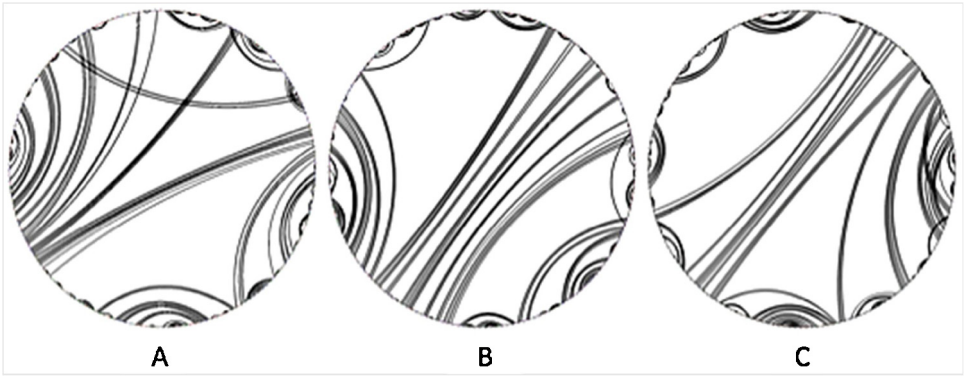

Fig. 3. Circular presentation of Pseudoknots in ERM transcripts, cross arcs indicated that structure is Psudoknotted. (A) *Ezr*, (B) *Rad*, (C) *Msn*.

Table 1
Sequences of primers for *Msn, Ezr*, *Rad* and gapdh for qRT-PCR.

Gene ID	Primer's Sequence (5'- 3')	Amplicon size
GAPDH	'5- CCCCTTCATTTGACCCTCAACTAC -3'	**250**
	'5- CCTTTTGGCTCCACCCTT -3'	
Msn	'5- TGAGCAGGATGAGAATGGAG -3'	**137**
	'5- AAGTAAGGGCCTTCAGATGC -3'	
Ezr	'5- GAGGGATGCTCAAGGACAGT -3'	**121**
	'5- ACTCCAAGCCAAAGGTCTGT -3'	
Rad	'5- AGAAGAAGAGGCGAGAGACG -3'	**128**
	'5- CTGCTCGGAGAGCTCTTTCT -3'	

much importance in brain tissue development. However, *Msn* was only visible in the early embryonic stage, in later stages its non-responsive fold alteration persisted, making its curial basal expression which is quite comparable to GAPDH (housekeeping gene). RNA molecules serve as mediators in determining the transcription level of genes. Three dimensional configuration of a transcript is based on its secondary structure, which is determined by the nucleotide base pairing. Basic stem and loop based structure of many RNA molecules is furnished with psudoknotes such as ribosomal RNAs, the catalytic core of group I introns, RNase P RNAs, and viral RNAs. Presence of psudoknots in RNA transcript has diverse impact on the integrity and stability of molecules, which directly effect on many processes including ribosomal frameshifting, regulation of translation and splicing, and gene expression (Ren et al., 2005). Thus, secondary RNA's transcript's structures of ERM greatly support our observation of *Ezr* and *Rad*'s transcript behaviour, in comparison to *Msn*, where *Rad* and *Ezr* elucidated instability with a least psudoknotted structures. These finding directly contributes towards co-relation of mRNA expression profile of *Ezr* and *Rad* to its RNA secondary structures.

On a conclusory note, the levels of all ERM members were found important for normal brain development of *Mus musculus*. The role of *Msn* and *Ezr* were observed in embryonic and primary postnatal stages which helps in brain tissues development whereas *Rad* helps in the maturation of brain tissues along with *Msn* and *Ezr*.

4. Materials and methods

4.1. Ethical statement

Animal care and experimental procedure were carried out in accordance with ethical review board (ERB) of Forman Christen College Lahore (FCCU), Pakistan and all the efforts were made to minimize the animal suffering. Animals were dissected under general anesthetic conditions and brain tissues were surgically separated.

4.2. Animal care and usage

In the present study, C57/B6 mice were used for experimental procedures. Breeding and housing conditions were highly standardized, facilitating a reliable environment. Durable cages were used, resistant to heat and chemicals. Nutritionally adequate diet was provided to mice. Temperature maintained at 24C and humidity level was between 50–70%. For each pregnant mice housing was single and for postnatal mice, it was group housing. Five pregnant mouse with 8–10 embryos were used, total 40–45 embryos were utilized for the study of each developmental stage.

4.3. Isolation of brain tissue and total RNA extraction

The day of vaginal plug detection was determined as first gestational day E.05. E10.5, E14.5 and E18.5 stages were identified on the bases of the plug dates. Developmental stages were chosen in according to data available from Mouse Atlas of Gene Expression (http://www.mouseatlas.org). Pregnant mice with specific embryonic days were anaesthetized by intraperitoneal injection of isoflurane (2-chloro-2-(difluoromethoxy)-1, 1, 1-trifluoroethane). Anaesthetized mothers were operated and embryos were separated from their uterine horns in 25 mM phosphate buffer saline medium. Whole brain tissues were isolated and immediately processed for RNA extraction using TRIzol reagent (Sigma) according to manufacturer's instructions. RNA qualitative and quantitative analyses were done on Nanodrop 2000 (Thermo scientific) of all RNA samples.

4.4. Primer designing and cDNA synthesis

Primers used for the amplification of target cDNA were designed from cross exon regions of sequences (NC_000086.7, NC_000083.6, NC_000075.6 and NC_000072.6) available in databank (www.ncbi.nlm.nih.gov). All sequences were aligned using clustalW (www.ebi.ac.uk/Tools/msa/clustalw2/) and primers (Table 1) were designed with the help of primer designing tool of the National Centre for Biotechnology Information databank (http://www.ncbi.nlm.nih.gov/tools/primer-blast/). Freshly prepared total RNA was used for first strand cDNA synthesis. 1 µg of total RNA was used to prepare the cDNA library by using oligodt and M-MLV reverse transcriptase (Thermo scientific #K1631) according to manufacturer's protocol. The presence of transcripts by conventional polymerase chain reaction. Reaction mixture (25 µl) was prepared by adding 1 µl of first strand cDNA, 2.5 µl 10x Taq buffer (Thermo scientific), 2 µl MgCl2 (2.5 Mm), 2 µl dNTP mix (2.5 mM), 2 µl forward primer (10µM), 2 µl reverse primer (10µM) (Table 1), 1.5 µl Taq Polymerase (1U). PCR analysis was carried out using thermocycler (Nyx Technik Amplitronyx Series 4 A4). The amplification conditions are as follows: initial denaturation at 94 ℃ for 3 min followed by 35 cycles of denaturation at 94 ℃ for 45 s, annealing at 58 ℃ for 30 s and extension at 72 ℃ for 1 min. Final extension was carried out at 72 ℃ for 7 min.

4.5. Secondary structure configuration of ERM transcripts

ERM member's mRNA transcripts sequences alignment was done using LocARNA web available server (http://rna.informatik.uni-freiburg.de/), by Bioinformatics Group at Department of Computer Science, Albert-Ludwigs-University Freiburg (Will et al., 2012, 2007; Smith et al., 2010). The prediction of RNA sequence homologies on the bases of LocARNA scores evaluates both sequence and structural similarity. RNA Secondary structures of ERM mRNA sequences were computed by using NUPACK RNA analysis software (www.nupack.org) by Caltech, California USA (Zadeh et al., 2011a; Dirks and Pierce, 2003, 2004; Zadeh et al., 2011b).

Pseudoknots configurations of the coding transcript were obtained using web available Probknot server (http://rna.urmc.rochester.edu/) developed and maintained by Methews labs at University of Rochester medical centre. For the evaluation of the predicted pseudoknots, pairs were found using an algorithm and each base pair is calculated accordingly (Reuter and Mathews, 2010; Mathews et al., 2010; Bellaousov and Mathews, 2010).

4.6. Quantification by real-time PCR

qRT-PCR was done for expression of moesin, ezrin and radixin transcript in brain tissues at various pre and post-developmental stages. Primers for qRT-PCR were designed on GenScript, an online tool for primer designing. Primer's specificity was determined by NCBI BLAST tool and moreover, manually. The relative expression fold difference of genes was calculated using ΔΔCT value calculations. The reaction conditions were optimized by determining the primer concentrations. The qPCR analysis was performed in CFX96 Real-Time PCR (Bio-Rad) using SYBER Green 1 mix. The reaction mixture was comprised of components from qPCR kit for SYBER Green 1 (Thermo Scientific

fermentas), both forward and reverse primers and 1 u l of diluted cDNA, GAPDH was used as housekeeping gene (Glare et al., 2002). All samples were used in triplicates. The cyclic conditions for qPCR, Initial denaturation at 94 °C for 5 min. Total thirty five cycles were adjusted on optimized thermocycling condition, denaturation was again at 94 °C for 45seconds, annealing at 58 °C for 15seconds whereas extension was at 72 °C for 45seconds. The final extension was given at 72 °C for 5mintues. Data was statistically analyzed by One way ANOVA and transcriptional expression difference were studied by ΔΔCT value analysis.

Author contributions

All authors have contributed equally towards this study.

Funding

This research did not receive any specific grant from funding agencies in the public, commercial, or not-for-profit sectors.

Conflicts of interest

The founding sponsors had no role in the design of the study; in the collection, analyses, or interpretation of data; in the writing of the manuscript, and in the decision to publish the results.

Acknowledgments

Forman Christian College (A Chartered University), Biological Science departmental funds were used to conduct this study. No external funding or grants were used to conduct this study neither for its publication.

References

Amieva, M.R., Wilgenbus, K.K., Furthmayr, H., 1994. Radixin is a component of hepatocyte microvilli in situ. Exp. Cell Res. 210, 140–144.
Bellaousov, S., Mathews, D.H., 2010. ProbKnot: fast prediction of RNA secondary structure including pseudoknots. RNA 16, 1870–1880.
Bretscher, A., 1983. Purification of an 80,000-dalton protein that is a component of the isolated microvillus cytoskeleton, and its localization in nonmuscle cells. J. Cell Biol. 7, 425–432.
Dirks, R.M., Pierce, N.A., 2003. A partition function algorithm for the nucleic acid secondary structure including pseudoknots. J. Comput. Chem. 24, 1664–1677.
Dirks, R.M., Pierce, N.A., 2004. An algorithm for computing nucleic acid base-pairing probabilities including pseudoknots. J. Comput. Chem. 25, 1295–1304.
Glare, E., Divjak, M., Bailey, M., Walters, E., 2002. β-actin and GAPDH housekeeping gene expression in asthmatic airways is variable and not suitable for normalising mRNA levels. Thorax 57 (9), 765–770.
Goldman, R.D., Grin, B., Mendez, M.G., Kuczmarski, E.R., 2008. Intermediate filaments: versatile building blocks of cell structure. Curr. Opin. Cell Biol. 20, 28–34.
Johnson, M.W., Miyata, Hajime., Vinters, H.V., 2002. Ezrin and moesin expression within the developing human cerebrum and tuberous sclerosis-associated cortical tubers. Acta Neuropathol. 104, 188. http://dx.doi.org/10.1007/s00401-002-0540-x.
Liao, G., Mingle, L., Water, L., Liu, G., 2015. Control of cell migration through mRNA localization and local translation. Wiley Interdis. Rev.: RNA 6 (1), 1–15.
Loebrich, S., Bähring, R., Katsuno, T., Tsukita, S., Kneussel, M., 2006. Activated radixin is essential for GABAA receptor alpha5 subunit anchoring at the actin cytoskeleton. EMBO J. 25, 987–999.
Louvet-Vallée, S., 2000. ERM proteins: from cellular architecture to cell signaling. Biol. Cell 92, 305–316.
Madan, R., Brandwein-Gensler, M., Schlecht, N.F., Elias, K., Gorbovitsky, E., Belbin, T.J., Mahmood, R., Breining, D., Qian, H., Childs, G., Locker, J., Smith, R., Haigentz, M., Gunn-Moore, F., Prystowsky, M.B., 2006. Differential tissue and subcellular expression of ERM proteins in normal and malignant tissues: cytoplasmic ezrin expression has prognostic significance for head and neck squamous cell carcinoma. Head Neck 28, 1018–1027. http://dx.doi.org/10.1002/hed.20435.
Mathews, D.H., Moss, W.N., Turner, D.H., 2010. Folding and finding RNA secondary structure. Cold Spring Harb. Perspect. Biol. 2 (12(December)), a003665.
Ren, J., Rastegari, B., Condon, A., Hoos, H.H., 2005. HotKnots: heuristic prediction of RNA secondary structures including pseudoknots. Rna 11 (10(October)), 1494–1504.
Reuter, J.S., Mathews, D.H., 2010. RNAstructure: software for RNA secondary structure prediction and analysis. BMC Bioinform. 11, 129.
Sarrió, D., Rodríguez-Pinilla, S.M., Dotor, A., Calero, F., Hardisson, D., Palacios, J., 2006. Abnormal ezrin localization is associated with clinicopathological features in invasive breast carcinomas. Breast Cancer Res. Treat. 98, 71–79.
Smith, C., Heyne, S., Richter, A., Will, S., Backofen, R., Freiburg, 2010. RNA tools: a web server integrating IntaRNA, ExpaRNA and LocARNA. Nucl. Acids Res. 38 (Suppl), W373–377.
Thomas, Risler., 2011. Cytoskeleton and cell motility. arXiv 1105, 2423R.
Valderrama, Ferran., Thevapala, Subangi, Ridley, Anne J., 2012. Radixin regulates cell migration and cell-cell adhesion through Rac1. J. Cell. Sci. 125, 3310–3319. http://dx.doi.org/10.1242/jcs.094383.
Will, S., Joshi, T., Hofacker, I., Stadler, P., Backofen, R., 2007. Inferring non-coding RNA families and classes by means of genome-scale structure-based clustering. PLoS Comput. Biol. 3 (no. 4), e65.
Will, S., Joshi, T., Hofacker, I., Stadler, P., Backofen, R., 2012. LocARNA-P: accurate boundary prediction and improved detection of structural RNAs. RNA. 18 (no. 5), 900–914.
Yaming, Jiu., Jaakko, Lehtimäki., Sari, Tojkander., Fang, Cheng., Harri, J.äälinoja., Xiaonan, Liu., Markku, Varjosalo., John, E., Pekka, Lappalainen, 2015. Bidirectional interplay between vimentin intermediate filaments and contractile Actin stress fibers. Cell Rep. 10, 1511–1518.
Younghyeb, Moon., Joo Yeona, Kim., Yoena, So, Choi, Kyungjinb, Kim., Hyuna, Kim., Woong, Sun., 2011. Induction of ezrin–radixin–moesin molecules after cryogenic traumatic brain injury of the mouse cortex. Neuroreport 22 (6), 304–308.
Zadeh, J.N., Steenberg, C.D., Bois, J.S., Wolfe, B.R., Pierce, M.B., Khan, A.R., Dirks, R.M., Pierce, N.A., 2011a. NUPACK: analysis and design of nucleic acid systems. J. Comput. Chem. 32, 170–173.
Zadeh, J.N., Wolfe, B.R., Pierce, N.A., 2011b. Nucleic acid sequence design via efficient ensemble defect optimization. J. Comput. Chem. 32, 439–452.